

A DIGITAL METHOD FOR THE COMPENSATED MOLD DESIGN OF COMPOSITE PARTS

Elias DELSOL¹⁻², Ismail TAOUIL¹⁻², Wiyao AZOTI¹, Bruno CASTANIE¹, Philippe OLIVIER¹ & Léon RATSIFANDRIHANA²

¹Institut Clément (ICA), Université de Toulouse, CNRS UMR 5312, INSA, ISAE-Supaéro, INSA, IMT Mines Albi, UPS, France

²SEGULA AEROSPACE & DEFENCE, SEGULA TECHNOLOGIES, Immeuble EQUINOX, Bat-1, 24 Boulevard Déodat de Séverac, 31770 Colomiers, France

Abstract

Autoclave curing of composite parts involves multiphysical mechanisms causing residual deformation. Respecting the geometric tolerances of the part can constitute a real challenge, and requires the design of a compensated mold. The objective of this study carried out on composite plates is to develop a digital mold design method. Therefore, a tool predicting curing behavior developped in previous studies was used. This is coupled with a method for calculating the shape of the compensated mold. This method is applied on a thick plate and on the thin fabricated plate in order to study the convergence of the optimization problem in both cases. The correction method thus studied is efficient on thick plates, but has some convergence issues on thin plates because of non-linearities.

Keywords: Virtual manufacturing, compensated mold, warpage, spring-in

1. General introduction

Composites materials takes an important place in the aeronautical industry [1]. The manufacture of thermosetting composite parts in an autoclave, reserved for parts with high mechanical performance, involves complex multi-physicals mechanisms. The consequence is the formation of residual stresses affecting the mechanical behavior and geometry of the part. In this paper, a simple case study with a non symmetric stacking [0,90,0, 90] is studied both experimentally and numerically. Then a simple linear procedure is applied to get a compensated mold from a numerical point of view.

1.1 Thermoset curing multiphysic mechanisms

A composite part curing in an autoclave is the site of multiphysical mechanisms causing residual deformations, often called PID (Process Induced Deformations) [2]. As a consequence, a part never has the exact shape of the mold [3, 4]. There are a large number of mechanisms, with varying influences.

The first mechanism is thermal expansion mismatch between the fiber and the resin. The differential of thermal expansion creates stresses at the fiber/resin interface. In fact, on the microscopic scale, a Von-Mises residual stress of about 30 MPa forms during cooling of 100 °C [5]. However, these constraints do not always materialize through the formation of residual deformations. In the case of a plate with a symmetric lay-up, there is not warping due to this phenomenon. For more complex parts, this mechanism results in PID matching, even with symmetrical lay-up [5].

A second mechanism is chemical shrinkage. The polymerization of the resin is accompanied by a reduction in its volume. This phenomenon varies depending on the type of resin, but for epoxy resign, a reduction of 7% in the volume of resin is observed [6]. This phenomenon is complicated by the

anisotropy of a composite material, since this shrinkage mainly generates deformations in the transverse direction. From a mechanical point of view, the consequences of this mechanism are similar to the fiber/matrix thermal expansion mismatch.

Thermal gradients in the part also cause residual stresses. Indeed, during convection heating of the part in the autoclave, thermal gradients appear [7]. Additionally, polymerization is an exothermic reaction, which contributes to the appearance of non-uniformity in the temperature distribution in the part. This mechanism complicates the behavior of the part during the cure and leads to the appearance of residual deformations. Indeed, the non-uniformity of the temperature distribution may causes property gradients in the part.

The tool/part interaction is also a source of residual deformation [8, 9]. Indeed, it is observed on thin plates with symmetrical layup of residual deformations, although the preceding mechanisms have no consequences. During curing, the differential in expansion between the mold and the part, coupled with the effects of environmental products, generates a frictional interaction leading to the deformation of the ply close to the mold. These deformations are fixed during the hardening of the resin, and cause bending.

1.2 Parameters

The mechanisms at work in the formation of deformations arise, in large part, from interactions between materials with different properties. Their influence varies according to a large number of parameters. They are classically classified into two categories: intrinsic to the part and extrinsic, a representation is proposed on the figure 1.

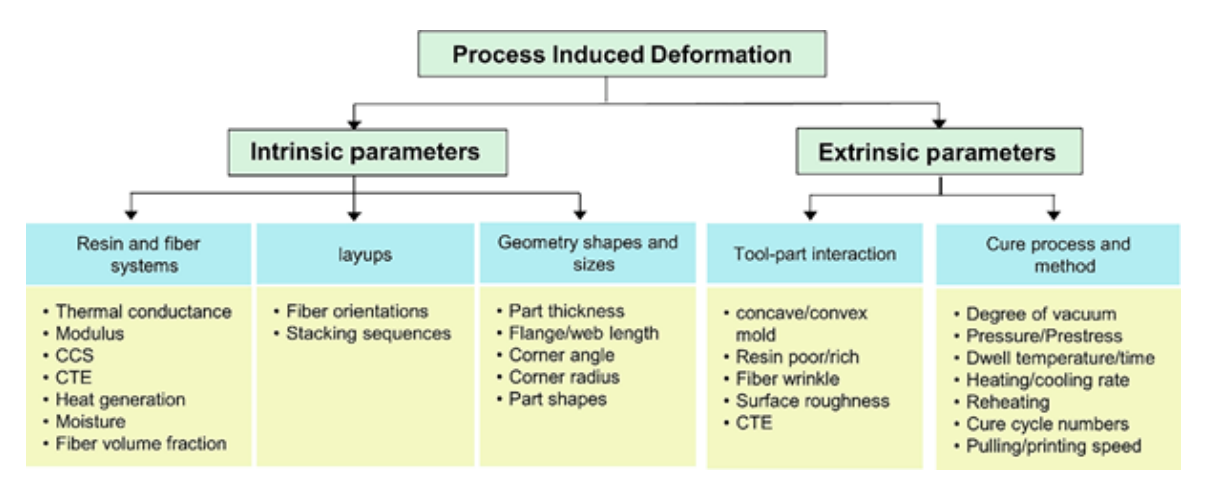


Figure 1 – Influence parameters of the PID [2]

1.3 Physical models

Multi-physical mechanisms are at work during curing. They lead to the formation of residual stresses, which can, depending on the state of various parameters, cause residual deformations. It is appropriate to model its behavior with a view to predicting deformations.

First, the temperature distribution in the part is described by the heat equation. It is characterized by the addition of a term linked to the exothermic nature of the polymerization.

$$\rho_{c}C_{p}\frac{\partial T}{\partial t} = div(\lambda.grad(T)) + \rho_{m}H_{tot}V_{m}\frac{d\alpha}{dt}$$
(1)

 ρ_c the density of the composite, C_p the specific heat at constant pressure of the composite, T the temperature, t the time, λ the thermal conduction coefficient, ρ_m the density of the resin and α the

progress of the polymerization and H_{tot} the total enthalpy of reaction.

For the kinetics of the chemical reaction, various models exist. Generally, phenomenological type models are used, in particular that of Kamal and Sourour [10].

$$\frac{d\alpha}{dt} = (k_1 + k_2 \alpha^m)(\alpha_{max} - \alpha)^n$$
 (2)

$$k_i = A_i e^{-\frac{E_{a_i}}{RT}} \tag{3}$$

 α is the degree of cure, α_{max} the maximum degree of cure. m, n and A_i are constants. R is the universal gaz constant and E_{a_i} is the activation energy.

From the knowledge of the polymerization rate and the temperature, it is possible to model the phase changes of the resin. During curing, the resin goes from a viscous state to a glassy state through a rubbery phase. The first phase change occurs at a precise polymerization rate denoted α_{gel} . The transition to the glassy state occurs when the temperature of the resin reaches the glass transition temperature, denoted T_g . The most used model to calculate T_g is that of Di-Benedetto [11].

$$T_g = T_{g_0} + \frac{\lambda_{T_g} \alpha (T_{g_\infty} - T_{g_0})}{1 - (1 - \lambda_{T_g}) \alpha} \tag{4}$$

 T_{g_0} the glass transition temperature for $\alpha=0$, T_{g_∞} the glass transition temperature for $\alpha=1$ and λ_{T_g} the glass transition factor mobility of chains.

Finally, the phase in which the resin is makes it possible to express the evolution of the mechanical behavior of the laminate during curing. Different models exist, with varying complexities. The CHILE (Cure Hardening Instentaneous Linear Elastic) model is often used to model the mechanical behavior of the material. Initially proposed by Bogetti and Gillespie [12], this model considers that the resin has a linear elastic behavior with an instantaneous stiffness model depending on the polymerization rate. A classic version of the model is proposed on the equation (5) [13]. For modern resins, such as IMA/M21EV, a modification of the model is necessary [7, 14].

$$E(T_g) = \begin{cases} E_1 & \text{si } T^* < T_{C1}^* \\ E_1 + \frac{T^* - T_{C1}^*}{T_{C1}^* - T_{C2}^*} (E_2 - E_1) & \text{si } T_{C1}^* \le T^* < T_{C2}^* \\ E_2 & \text{si } T^* \ge T_{C2}^* \end{cases}$$
(5)

 $T^* = T_g - T$, E_2 and E_1 are respectively the relaxed and un-relaxed modulus.

1.4 Deformation prediction

The prediction of residual deformations is generally carried out by a complete simulation of the curing. A classic prediction tool is composed with three modules [2]:

- thermokinetics to obtain the distribution of temperature and reticulation rate in the room,
- fluid mechanics, to simulate the behavior of the laminate before gelation,
- thermomechanical, to simulate the mechanical behavior of the part after gelation.

However, other models exist, and do not take into account the fluid mechanics part because the impact of the resin flow is considered negligible [7].

2. Prediction study on thin plates

The choice of thin plates over thick ones for this study, especially with a non-symmetric stacking sequence, is explained by the fact that they exhibit more pronounced residual deformation behavior due to the major deformation mechanisms: thermal expansion, chemical shrinkage, and tool-part interaction.

2.1 Study case

Four similar 250×250 mm² thin composite plates were manufactured using AS4/8552 carbon/epoxy prepreg laminates produced by Hexcel. These composite laminates were cured and bonded through an autoclave process, and residual deformation fields were measured using Digital Image Correlation (DIC).

2.1.1 Experimental procedure

- Stacking sequence: each plate is composed of four laminates with a non symmetric stacking sequence of [0,90,0,90]. Each laminate is of 0.18 mm cured thickness.
- Autoclave molding assembly: the four samples are placed on an aluminium mold, and a vacuum bagging system is applied. The figure 2 emphasizes the sequence used in this study.
- Curing Cycle: The composite laminates are introduced into the autoclave and cured using a two-dwell temperature cycle at 110°C and 180°C, respectively, accompanied by a pressure cycle at 7 bar and a compaction pressure of 0.2 bar.

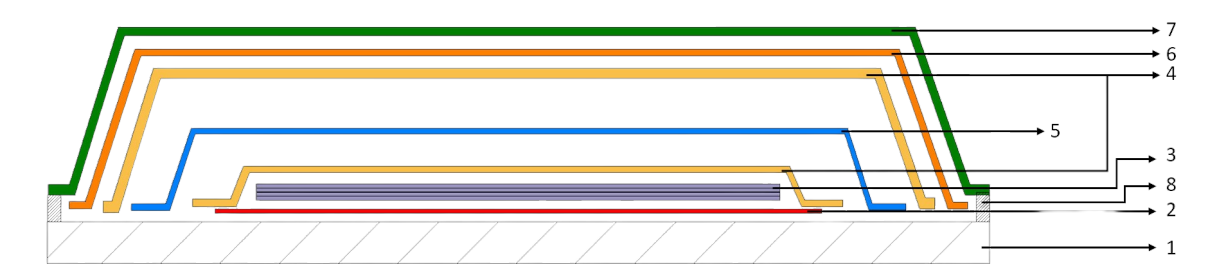


Figure 2 – Autoclave molding assembly

Reference	nce Designation			
1	Aluminium Mold			
2	Peel Ply			
3	Composite Part			
4	Non perforated Release Film			
5	Bleeder ply			
6	Breather ply			
7	Vacuum Bag			
8	Sealant Tap			

Table 1 – Components used in the autoclave process

2.2 Experimental results

After cooling the plates to room temperature, an rapid deformation takes place immediately upon removing the bagging system, specifically when the vacuum pressure is eliminated. Primary observations show that the plates present a cylindrical shape with a single k_{0x} curvature, and they are by-stable, meaning that they also present a single curvature k_{0y} , if forced to the opposite direction. Far away from the results predicted by the classical laminates theory, which presents both k_{0x} and k_{0y} curvatures. This phenomenon is common with non-symmetric thin composite plates and has been addressed in several studies [15, 16, 17, 18, 19].

Dimensional control of deformations involves measuring the displacements undergone by parts. Digital Image Correlation (DIC) was used to measure the out-of-plane deformation of all samples and indicates its amplitude across the entire surface.

2.2.1 Experimental setup

Two AVT PIKE F-505B cameras with 5 megapixel resolution (image size 2452 (H) x 2054 (V)) were used to capture the images. Technically, two cameras were needed to form and analyze the 3D shape. Calibration plate photos were taken for calibration with different locations and angle adjustments (see figure 3).

Analysis are carried out on the basis of the intensity of the black dots patterns (speckles) applied to the surface of the samples. As all laminates are black, a layer of white color was required to produce a random black pattern on a top surface. Two coats of white were sprayed on top of the laminate surface. A roller with dots size of 0.026mm was used to produce the pattern. Four layers of speckle were applied to the laminate surface, two along the medians and two along the diagonals, in a direction perpendicular to each other (see Figure 4).

2.2.2 Dimensional control results

Figure 5 presents the results for the four plates obtained through DIC measurements. Each image captures the out-of-plane displacement (along the z-direction). The color scale indicates the magnitude of displacement, clearly showing the consistent single curvature deformation across the four samples.



Figure 3 – Experimental setup

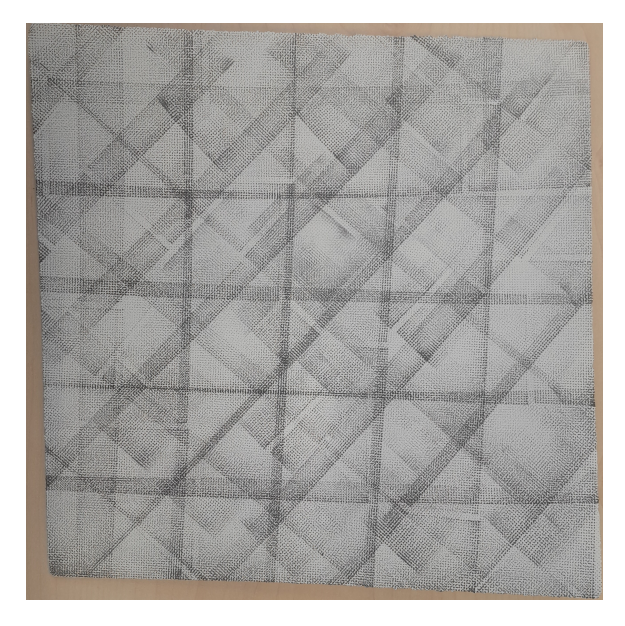


Figure 4 – Speckles pattern

Upon visual comparison of the DIC results, the difference between the maximum and minimum out-of-plane displacements was calculated for each plate. This metric serves as a quantitative measure of the flatness of the plates post-deformation. Figure 6 displays the flatness measurements for the plates labeled as "Plate-C1_Ass90_01" to " Plate-C1_Ass90_04". All four plates exhibit closely similar flatness with values around 10 mm, with a range of 1.25mm and a standard deviation of 0.61mm, which proves the consistent outcome across all controlled samples.

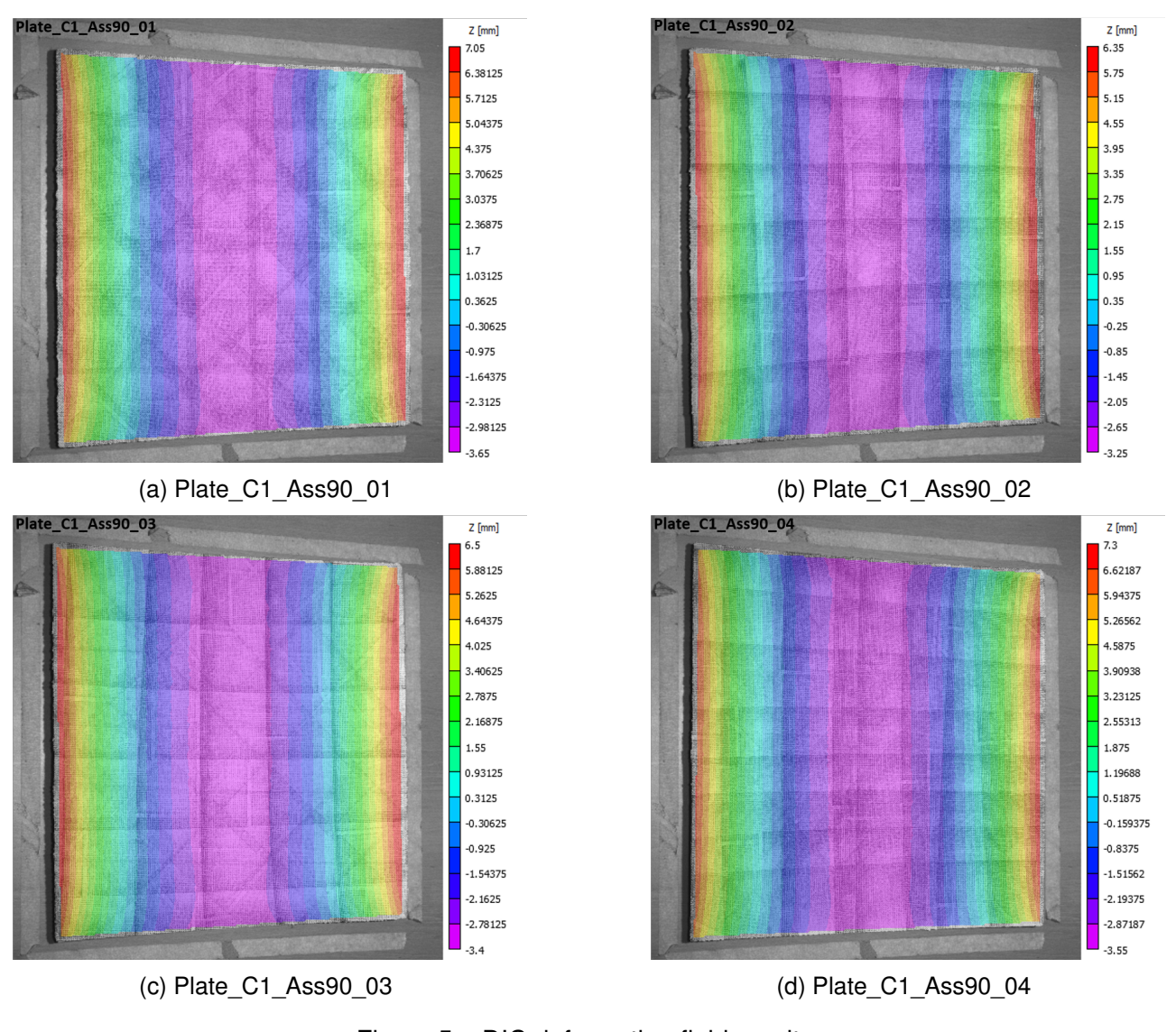


Figure 5 – DIC deformation field results

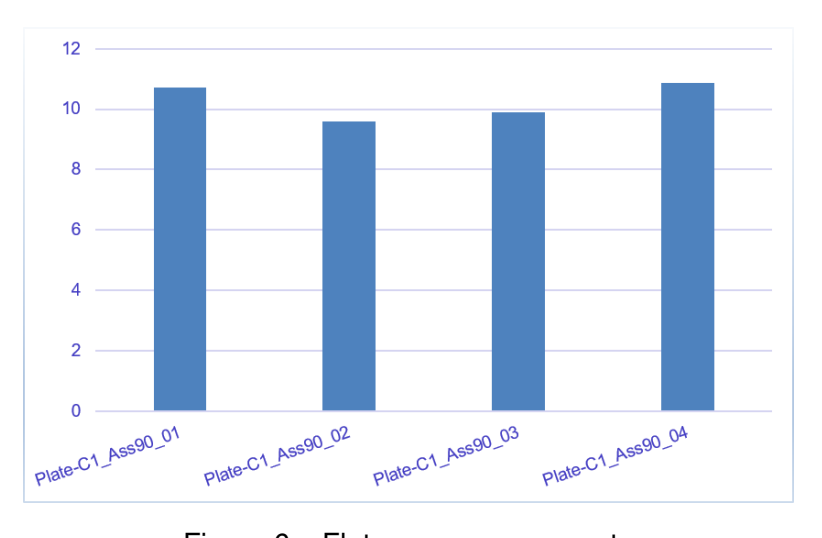


Figure 6 – Flatness measurements

2.3 Deformations prediction

The prediction of residual deformations was done using the previous work of L. Moretti [7, 14], by calculating the degree of cure first based on the cure kinetics model (6) and cure cycle temperature. Then the results are then fed into the mechanical analysis based on the mechanical properties (Table 2). ABAQUS software coupled with Fortran subroutines UMAT and UEXPAN were used to solve the problem. Furthermore, as mentioned previously, the simulation of residual deformations on thin plates requires a non-linear analysis [15]. To do this, the NLGEOM parameter is activated when simulating the demolding of the part.

2.3.1 Material Properties

Material properties for this study were derived from literature, mechanical properties (Table 2) and cure kinetics model constants (Table 3) were based on the studies of Nuri Ersoy [20, 21].

Mechanical properties

Property	Unit	Rubbery	Glassy
$\overline{E_{11}}$	MPa	165	134000
$E_{22} = E_{33}$	MPa	165	9480
$G_{12} = G_{13}$	MPa	44.3	5490
G_{23}	MPa	41.6	3272
$v_{12} = v_{13}$	-	0.346	0.271
<i>v</i> ₂₃	-	0.982	0.448
$lpha_{22}$	$\mu arepsilon$ / $^{\circ}$ C	-	40.0
$arepsilon_{22}^{cure}$	%	0.45	-

Table 2 – AS4/8552 mechanical properties [20]

• Cure kinetics Model

$$\frac{\mathrm{d}\alpha}{\mathrm{d}t} = \frac{A\mathrm{e}^{(-\Delta E/RT)}\alpha^m(1-\alpha)^n}{1 + \mathrm{e}^{C(\alpha - \alpha_{\mathrm{CO}} - \alpha_{\mathrm{CT}}T)}} \tag{6}$$

$$T_g = 164.6\alpha^2 + 51.0\alpha + 2.67\tag{7}$$

Constant	Value	Unit	Comments
E_a	65000	J/gmol	Activation energy
Α	7.00×10^{-4}	s^{-1}	Cure rate coefficient
m	0.5	_	First exponential constant
n	1.5	_	Second exponential constant
R	8.314	J/mol/K	Gas constant
С	30		Diffusion constant
$lpha_{CT}$	5.171×10^{-3}	K^{-1}	Constant accounting for increase in
			α_C with temperature
α_{C0}	-1.5148×10^{-3}	_	Critical degree of cure at T = 0K

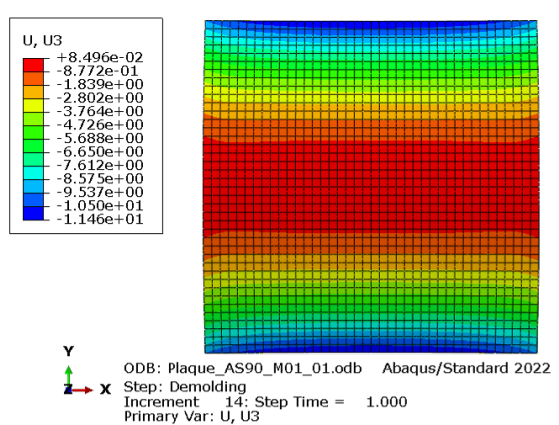
Table 3 – Key constants and their values related to the cure kinetics [21]

2.3.2 Simulation results

In the simulation procedure adopts a progressive approach, composed of three different case:

1. **Cooling simulation**: the simulation focuses on the cooling stage, considering constant mechanical properties of the composite part.

- 2. **Full cure cycle simulation**: the simulation considers a complete coupling between the mechanisms and the different evolution of the hardening parameters.
- 3. **Tool-Part interaction**: this simulation introduced the interaction between the tooling and the composite part, by considering a bonding between the peel ply and the plate, and a frictional interaction between the mold and the peel ply (the friction coefficient is set to 1).





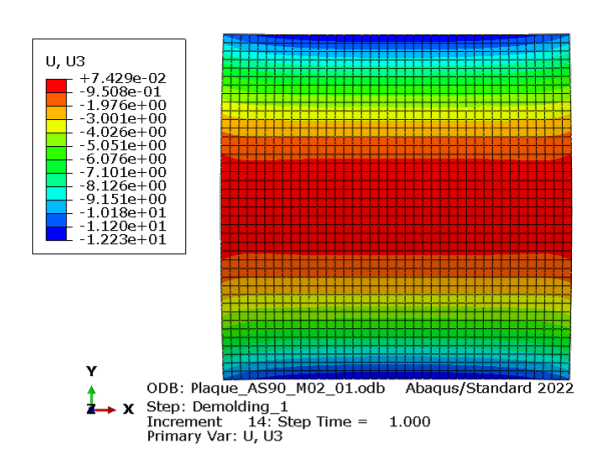


Figure 8 – U3 values for second simulation case

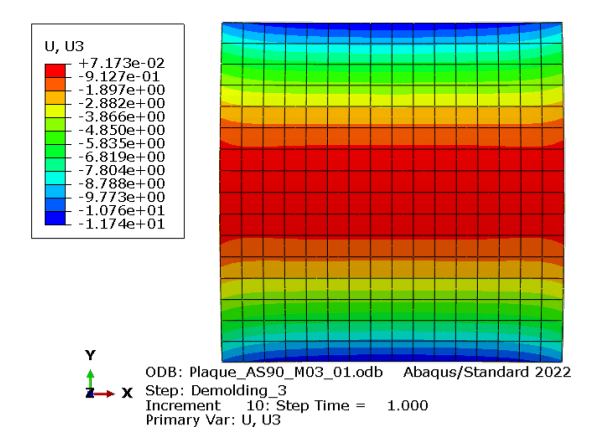


Figure 9 – U3 values for third simulation case

Figures 7, 8 and 9 show the out-of-plane deformations of the simulated part in the three cases. While the experimental results are obtained from the side that faced the mold, the simulation results show values from the opposite side, which explains the inverted shape represented with the color field. This indicates that the simulation produces the same deformed shape as the experimental results.

The simulations overestimate the residual deformations, but allow a correct prediction. Furthermore, we notice, in figure 10 that the first simulation allows a better prediction although the model used is the simplest. The increase in the predicted principal curvature between simulations 1 and 2 is not surprising insofar as an additional mechanism was added: chemical shrinkage. The addition of the part/tool interaction allows a reduction in residual deformations, this is consistent with the literature [7].

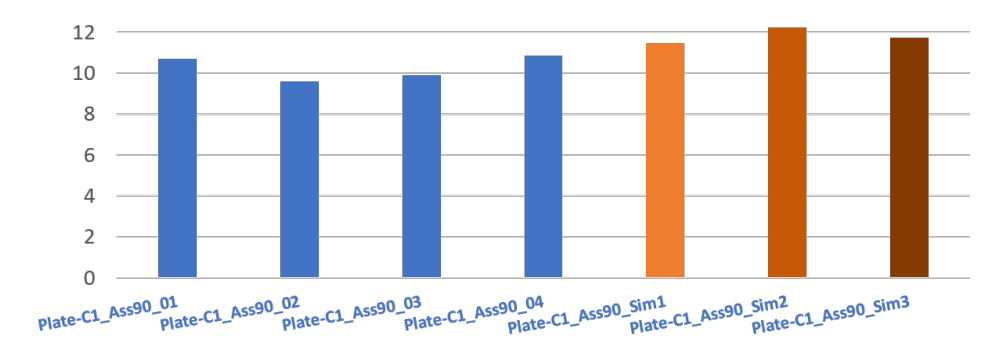


Figure 10 – Flatness Comparison between experimental and simulation cases

3. Compensation for residual deformations

3.1 Problem formulation

The development of a residual deformation simulation tool allows the design of the compensated mold, ideally, by eliminating experimental iterations. The shape of the compensated mold can be obtained through an optimization algorithm. Indeed, we consider the surfaces S_0 , S_1 , S_2 respectively the desired surface, the surface of the mold and the surface of the part in contact with the mold after demolding. The optimization problem is equivalent to calculating the surface S_1 so that S_0 and S_2 are the same. Since this optimization problem is vast, a restriction of the size of the problem will have to be carried out.

The optimization problem for the compensated mold designing is reduced to the optimization of a single parameter, called correction factor (noted c), which is strictly negative. A first simulation of curing with a non-compensated mold makes it possible to obtain the PID which must be compensated by the mold. This shape is meshed in such a way as to obtain 100 control points over the entire part surface. Then, the compensated mold shape is obtained by generating a surface from the 100 control points, only the z-coordinate is modified: it is multiplied by the coefficient c. In order to study the convergence of the problem, we consider two indicators, the flatness, and the sum of squares deviations between the initial and the final z-coordinate of the plate after curing.

3.2 Study Objectives

This study aims to study the relevance of reducing the dimension of the optimization problem. To do this, two plates are considered as presented in the table 4. The first plate is a 3.8 mm thick plate, so there is no problem of numerical instability associated with the large displacement. The other plate is the one studied in the previous part, so there is the problem associated with large displacements.

Number	Layup	Dimensions	Material
1	$\left[-45_2/45_2/-45_2/90_2/45_4/-45_2/0_2/45_2/-45_2\right]$	150 x 150	IMA/M21EV
2	[0, 90, 0, 90]	250 x 250	AS4/8552

Table 4 - Components used in the autoclave process

3.3 Application of the method

Concerning the first plate, the initial shape is presented in figure 11a. The initial flatness obtained with a flat mold is 1.68 mm. The optimization problem is indeed convergent, and the shape of the curve is a third-order polynomial, as shown in the figure 12. An optimum is found for c=-0.95 (see the figure 11c), the flatness is then 0.08 mm, it is thus divided by 20. The final shape of the part is different from the initial shape. Indeed, the more the shape of the compensated mold approaches the optimal shape, the more the shape of the final part deviates from that initially obtained.

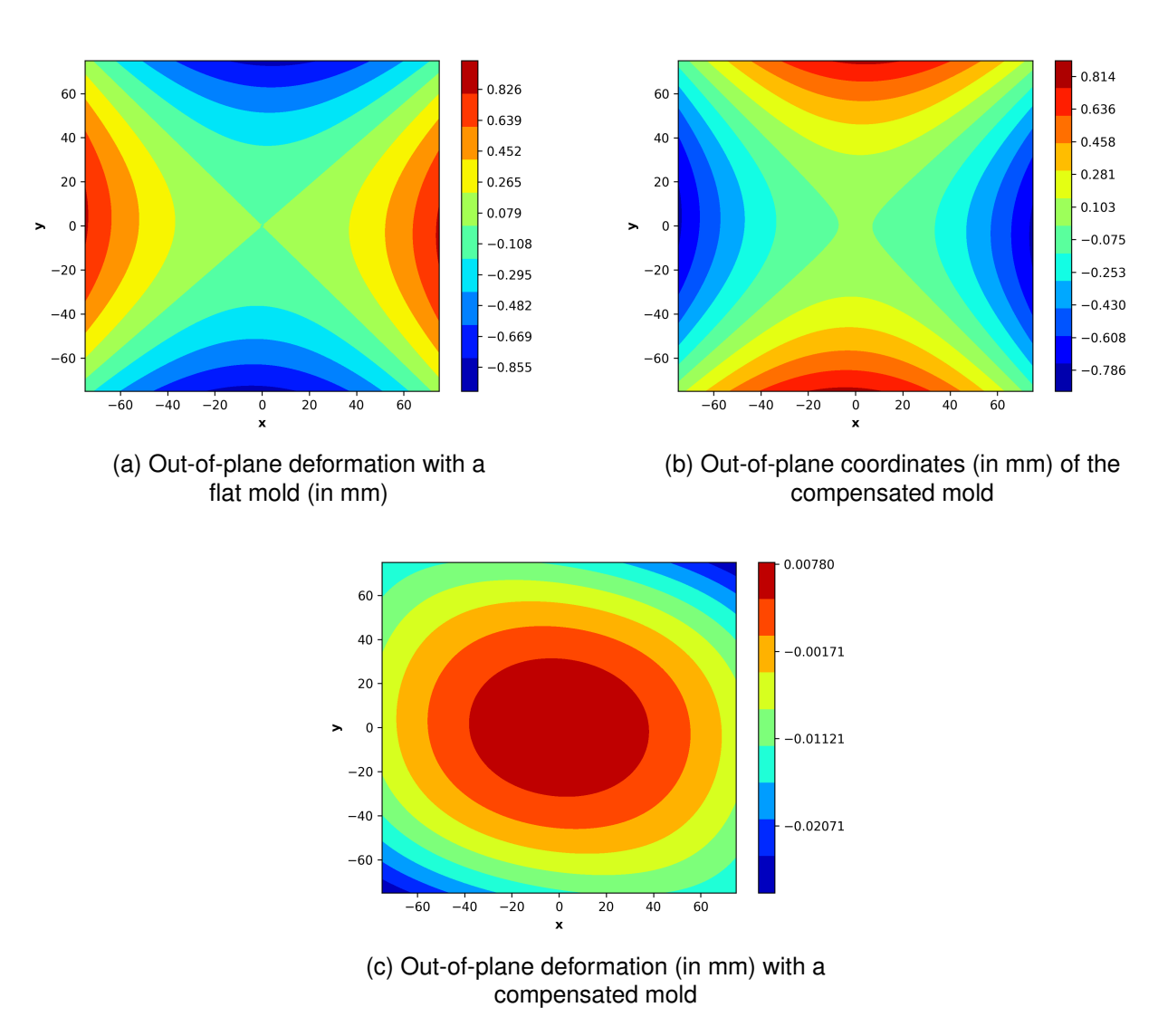


Figure 11 - Study of convergence on plate 1

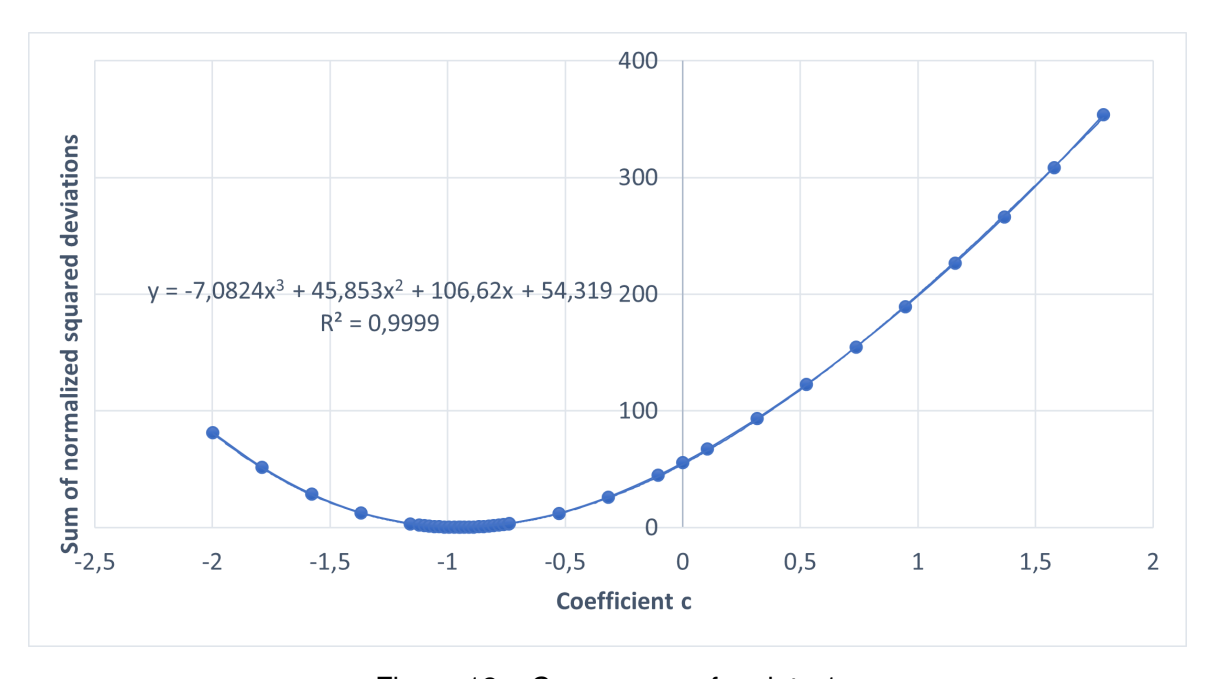


Figure 12 - Convergence for plate 1

The study of the convergence of the problem on plate 2 gives different results due to non-linearity. Figure 13 shows that the evolution curve of the objective function is noisy. The general appearance of the curve is similar to that of the study on a thick plate. However, thanks to a refinement between c=-1 and c=-0.5, we notice oscillations: the flatness of the plate obtained is included there. Between 2.6 mm and 11 mm. A numerical solution nevertheless emerges, presented in figure 14, the flatness is divided by 4.5. This result is clearly less good than for a thick plate, especially the noise on the solution makes uncertain the shape which could really be observed experimentally.

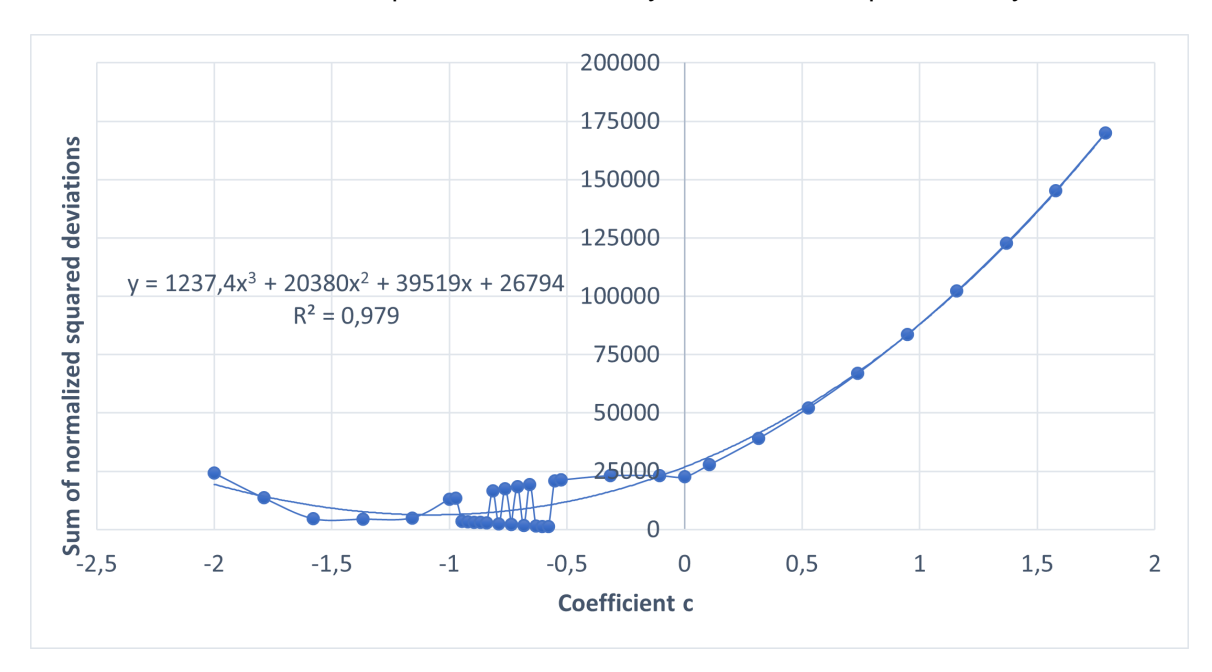


Figure 13 – Convergence for plate 2

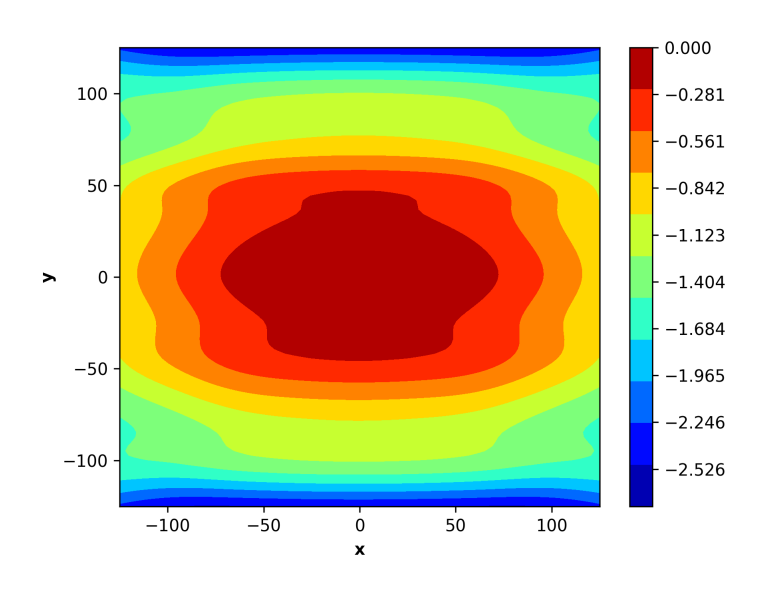


Figure 14 – Out-of-plane deformation (in mm) with a compensated mold for plate 2

4. Conclusions and perspectives

To conclude, an experimental study of residual deformations on thin plates was carried out. A prediction tool allows a prediction of the residual deformations on this case study. This takes into account the three main mechanisms at work in the formation of PIDs on thin plates, that is to say differential thermal expansion fiber/resin, chemical shrinkage and part/mold interaction. Finally, a simple one-parameter method for designing the compensated mold was proposed. This method is efficient for thick plates, but is much less effective on thin plates due to non-linearity.

Improvements to the prediction tool appear necessary to more precisely model the multiphysics counting of the part during the cure. In particular, the mechanical constitutive model consisting of only two modules with a sudden transition is oversimplified. Concerning the design method of the compensated mold, this must be verified experimentally. Additional studies must be carried out to take into account the effects of non-linearity on the design of the compensated mold.

5. Copyright Statement

The authors confirm that they, and/or their company or organization, hold copyright on all of the original material included in this paper. The authors also confirm that they have obtained permission, from the copyright holder of any third party material included in this paper, to publish it as part of their paper. The authors confirm that they give permission, or have obtained permission from the copyright holder of this paper, for the publication and distribution of this paper as part of the ICAS proceedings or as individual off-prints from the proceedings.

References

- [1] Bruno CASTANIE, Christophe BOUVET, and Malo Ginot. Review of composite sandwich structure in aeronautic applications. *Composites Part C: Open Access*, 1:100004, 2020.
- [2] Biao Wang, Shuaijie Fan, Jiping Chen, Weidong Yang, Weiping Liu, and Yan Li. A review on prediction and control of curing process-induced deformation of continuous fiber-reinforced thermosetting composite structures. *Composites Part A: Applied Science and Manufacturing*, 165:107321, 2023.
- [3] G Fernlund and A Poursartip. Getting part dimensions right in composites molding. *Compos World Article*, 2015.
- [4] Erik Kappel. Compensating process-induced distortions of composite structures: a short communication. *Composite Structures*, 192:67–71, 2018.
- [5] MR Wisnom, M Gigliotti, N Ersoy, M Campbell, and KD Potter. Mechanisms generating residual stresses and distortion during manufacture of polymer–matrix composite structures. *Composites Part A: Applied Science and Manufacturing*, 37(4):522–529, 2006.
- [6] Chun Li, Kevin Potter, Michael R Wisnom, and Graeme Stringer. In-situ measurement of chemical shrinkage of my750 epoxy resin by a novel gravimetric method. *Composites Science and Technology*, 64(1):55–64, 2004.
- [7] L. Moretti, P. Olivier, B. Castanié, and G. Bernhart. Experimental study and in-situ fbg monitoring of process-induced strains during autoclave co-curing, co-bonding and secondary bonding of composite laminates. *Composites Part A: Applied Science and Manufacturing*, 142:106224, 2021.
- [8] M Fiorina, A Seman, Bruno Castanié, KM Ali, C Schwob, and L Mezeix. Spring-in prediction for carbon/epoxy aerospace composite structure. *Composite Structures*, 168:739–745, 2017.
- [9] L Mezeix, A Seman, MNM Nasir, Y Aminanda, A Rivai, Bruno Castanié, Philippe Olivier, and KM Ali. Spring-back simulation of unidirectional carbon/epoxy flat laminate composite manufactured through autoclave process. *Composite structures*, 124:196–205, 2015.
- [10] MR Kamal and S Sourour. Kinetics and thermal characterization of thermoset cure. *Polymer Engineering & Science*, 13(1):59–64, 1973.
- [11] JP Pascault and RJJ Williams. Relationships between glass transition temperature and conversion: Analyses of limiting cases. *Polymer Bulletin*, 24:115–121, 1990.
- [12] Travis A Bogetti and John W Gillespie Jr. Process-induced stress and deformation in thick-section thermoset composite laminates. *Journal of composite materials*, 26(5):626–660, 1992.
- [13] Andrew A Johnston. *An integrated model of the development of process-induced deformation in autoclave processing of composite structures.* PhD thesis, University of British Columbia, 1997.

- [14] Laure Moretti, Bruno Castanié, Gérard Bernhart, and Philippe Olivier. Characterization and modelling of cure-dependent properties and strains during composites manufacturing. *Journal of composite materials*, 54(22):3109–3124, 2020.
- [15] Marco Gigliotti, Michael R. Wisnom, and Kevin D. Potter. Loss of bifurcation and multiple shapes of thin [0/90] unsymmetric composite plates subject to thermal stress. *Composites Science and Technology*, 64(1):109–128, January 2004.
- [16] Michael W. Hyer. Some Observations on the Cured Shape of Thin Unsymmetric Laminates. *Journal of Composite Materials*, 15(2):175–194, March 1981. Publisher: SAGE Publications Ltd STM.
- [17] Michael W. Hyer. Calculations of the Room-Temperature Shapes of Unsymmetric Laminatestwo. *Journal of Composite Materials*, 15(4):296–310, July 1981. Publisher: SAGE Publications Ltd STM.
- [18] Michael W. Hyer. The Room-Temperature Shapes of Four-Layer Unsymmetric Cross-Ply Laminates. *Journal of Composite Materials*, 16(4):318–340, July 1982. Publisher: SAGE Publications Ltd STM.
- [19] M. W. Hyer and Scott R. White. *Stress Analysis of Fiber-reinforced Composite Materials*. DEStech Publications, Inc, 2009. Google-Books-ID: qgTVpw_uACoC.
- [20] Nuri Ersoy, Tomasz Garstka, Kevin Potter, Michael R. Wisnom, David Porter, Martin Clegg, and Graeme Stringer. Development of the properties of a carbon fibre reinforced thermosetting composite through cure. *Composites Part A: Applied Science and Manufacturing*, 41(3):401–409, March 2010.
- [21] Nuri Ersoy, Kevin Potter, Michael R. Wisnom, and Martin J. Clegg. Development of spring-in angle during cure of a thermosetting composite. *Composites Part A: Applied Science and Manufacturing*, 36(12):1700–1706, December 2005.